



International Conference on Integrated Petroleum Engineering (IPE-2022)

Fabrication of nano Selenium in Solution plasma

Ha-Son NGO^{a*}, Huu-Thanh LE^b, Ngoc-Tuan TRAN^a

^aFirst affiliation, Address, City and Postcode, Country

^bSecond affiliation, Address, City and Postcode, Country

Abstract

Solution plasma process (SPP) is considered a novel method for the synthesis of nanomaterials using plasma discharge in liquid. The SPP, which is a non-equilibrium plasma, can provide an extremely rapid reduction of a metal ion to the neutral form without the presence of reducing agent. In this study, the Selenium nanoparticles (SeNPs) have been synthesized in solution plasma. The method is capable of fabricating selenium nanoparticles with the uniform size in water, and high stability without stabilizer. The synthesized selenium nanoparticles were characterized by UV-Visible Spectrophotometry (UV-vis), X-Ray Diffraction (XRD), Dynamic Light Scattering Particle Size Analyzer (DLS), Scanning Electron Microscope (SEM) and Transmission Electron Microscope (TEM) techniques. The results showed that the SeNPs were in uniform flower-like nanostructures with diameter ranging from 50 to 100 nm in ethanol/water mixture. The fabricated selenium nanoparticles reveal potential in antimicrobial and antioxidant applications

Keywords: Selenium nanoparticles (SeNPs) solution plasma, antioxidant, plasma discharge, antimicrobial property

1. Introduction

In the sciences of physics, chemistry, and biology, the element selenium (Se) is crucial. Selenium is naturally found in two different forms: inorganic (selenite and selenate) and organic (selenomethionine and selenocysteine). In nature, selenium can be found in both crystalline and amorphous polymorphism forms. The crystalline forms of selenium are monoclinic and trigonal. Se₈ ring-containing monoclinic selenium (m-Se) is red in hue. It exists in three allotropic forms based on various packings. The most stable crystalline form of selenium at ambient temperature is trigonal selenium (t-Se), which is dark in colour. The non-crystalline forms of selenium are vitreous selenium, black amorphous selenium, and red amorphous (a-Se) selenium (Zhu et al., 2019). Selenium, a component of selenoproteins and selenocompounds in the human body, is essential for metabolism, thyroid hormone, DNA synthesis, reproduction, and defence against oxidative stress and infections. There are numerous commercial and industrial uses for it. Because of its low melting point and high photoconductivity, it has excellent catalytic activity for organic hydration and oxidation processes. Selenium is a vital trace element for human health, yet there is a very thin line separating it from harm. Selenium needs for men and women should be 60 and 70 micrograms per day, respectively, according to the United Kingdom organisation of vitamins and minerals (Hariharan & Dharmaraj, 2020). Selenium is a vital biological component of glutathione peroxidase, an enzyme that functions as an antioxidant by protecting crucial SH-groups and breaking down peroxides. Due to its ability to catalyse the oxidation of intracellular thiols, which results in the death of microscopic organisms, selenium has bactericidal properties (Spallholz, 1994), (Sieber et al., 2005). Metal nanoparticles have an infinite number of uses in biomedicine thanks to the current growth in nanotechnology. Metal nanoparticles (Au and Ag) offer enormous medical advantages but are more expensive to synthesise, whereas Se nanoparticles (SeNPs) are affordable to synthesise and could be combined with other biological agents to improve their bioactivities. Because elemental Se is the least poisonous form of selenium, its nano-form has garnered considerable attention. Remarkably,

* Corresponding author.

E-mail address: author@institute.xxx.

functionalized SeNPs are less cytotoxic than other forms of selenium, including selenate, selenite, selenoproteins, and inorganic selenium. In clinical investigations, elemental nano-sized selenium could be a preferable alternative to traditional selenium supplies. SeNPs are extremely physiologically active (J. Zhang et al., 2005), anti-hydroxyl radicals (Gao et al., 2002), and chemopreventive agents (Wang et al., 2007), (J.-S. Zhang et al., 2001) that detoxify heavy metal exposure (Ikemoto et al., 2004) and reduce DNA damage (Huang et al., 2003). Solutions obtained by earlier manufacturing methods were commonly doped and contaminated. Presently, it is urgently necessary to look into a cutting-edge method for producing extremely pure nanoselenium. It's becoming increasingly popular to create nanoparticles using electrochemical synthesis techniques, particularly the solution plasma method. Solution plasma is an atmospheric nonequilibrium plasma that is created by electrical discharge in the liquid phase at ambient temperature. The plasma designs, solutions, electrode materials, and power supply characteristics are easily modifiable. A variety of product sizes, shapes, and compositions could be controlled thanks to these features of the solution plasma, making it beneficial for a variety of applications. One possible application is as a tool for the synthesis and modification of novel materials (Kim et al., 2015), (J. Zhang et al., 2017).

In this work, solution plasma technique was used to create selenium nanoparticles. As far as we are aware, this could be the first attempt to investigate the viability of synthesising nanoselenium and characterising the final product using this method.

2. Experimentals

2.1. Chemicals

The selenium dioxide SeO_2 99.99 % (Sigma-Aldrich) and the ethanol 96 % (China) were used as they were received from the source. The precursor of the selenium-containing acid H_2SeO_3 was made by diluting SeO_2 powder in double-distilled water to a concentration of 3mM. Without additional purification, H_2SO_4 , HCl , HNO_3 , NaOH , and oxides were used in the research. The experimental electrode is a 99.9% pure Tungsten (W) electrode with a 1mm diameter.

2.2. Reactor set-up

The reaction apparatus is a beaker with a silicon stopper and is mounted on a magnetic stirrer. The reaction system is built around a tungsten electrode system. A Pekuris high-frequency power supply provides the current, and an oscilloscope is used to check the stability of the current during plasma discharge. The electrode diameter is typically 1 mm, and the electrode spacing ranges from 0.5 to 2 mm. This is because a high current density (mA/cm^2) at the two electrodes is required to produce bright plasma from a plasma discharge.

2.3. Selenium nanoparticles synthesis

A 3mM concentration of H_2SeO_3 was made as a solution in water. Tungsten is used to make the metal electrode system in the reactor, which has electrodes that are 1.5 mm in diameter and spaced 0.5 mm apart. The electrodes are protected by a teflon tube that can withstand extreme temperatures. 2 kV input voltage, 20 kHz frequency, and a 2 s pulse width are employed. Distilled water and distilled water combined with ethanol are the systems utilised as solvents. After the reaction, the solution was kept at 5°C for additional research.

2.4. Product's characterizations

The elemental composition of the generated material was analysed using energy dispersive X-ray spectroscopy (EDX). X-ray diffraction spectroscopy and transmission electron microscopy (TEM) were utilised to further understand its structure and crystallinity. In order to understand the consistency of the generated nanoselenium, the particle size distribution was also investigated. EDX measurements and was obtained on Hitachi-S4800 (Japan). The material's UV-vis spectrum was recorded using a UV-Vis UH4150 Hatachi equipment (Japan). Also, a JEM 2100 High Resolution Transmission Electron Microscope was used to take TEM images of the product.

2.5. Effect of different parameters

2.5.1. Effect of solvent

One of the key elements in calculating the discharge potential of the solution is the conductivity of the solution. The discharge voltage will drop as the solution's conductivity rises. Additionally, the solvent system for the reaction has a significant role in the generation of free radicals. Some forms of free radicals might be advantageous for the reaction, while others can be harmful. As a result, it is important to do research and choose the best solvent

system for the reaction. The study performed surveys using distilled water and ethanol/distilled water as its two solvent systems.

2.5.2. Effect of electrode distance

The electrode distance directly impacts the discharge voltage throughout the synthesis process and has an influence on the discharge primer potential, migration of electrons, ions, free radicals, and metal ions. The resistance of the solution during plasma discharge is also regulated by the distance between the two electrodes. We carried out a study and assessed how the electrode distance affected the response process at distances of 0.5, 1, 1.5, 2, and 3 mm. The study then suggests a relationship between the electrode distance and the solution's discharge potential and the reaction process's outputs.

2.5.3. Effect of voltage

One of the crucial variables affecting the development of the plasma discharge current, the type of the plasma flow, the stability of the discharge process over time, and the rise in temperature throughout the reaction is the voltage parameter value at the two electrodes. In order to determine the ideal voltage for material synthesis, this study examines the impact of voltage value during plasma discharge.

3. Results and discussions

3.1. Solvent selection

- Water as solvent

The reaction mixture is 10 mM H_2SeO_3 , with voltage parameters of 2Kv, pulse width of 0.3 s, electrode spacing of 0.5 mm, and pH of 3.

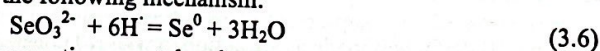
When a high voltage is applied to the two electrode plates, a strong electric field will appear. The electric field's influence causes the molecules to become ionised, colliding to form a plasma current. Plasma discharge produces free radicals like H, OH, and O in aqueous solutions.



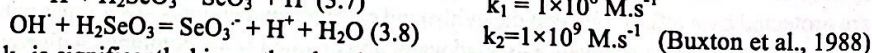
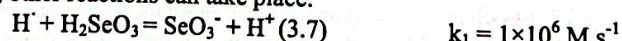
Recombination of free radicals:



The reduction process of Se^{+4} to Se^0 in solution solely involves free radicals $H\cdot$ when using distilled water as the solvent, according to the following mechanism:



However, in solution, other reactions can take place:



It was discovered that k_2 is significantly bigger than k_1 when the rate constants of the interaction between H free radicals and OH radicals with the H_2SeO_3 solution were compared. As a result, the reduction process of Se^{4+} to Se^0 does not occur in distilled water.

Figure 1 demonstrates that for the distilled water solvent system, the reaction solution does not change colour after the plasma discharge duration of 60 minutes, suggesting that no selenium nanoparticles are being formed in the solution.

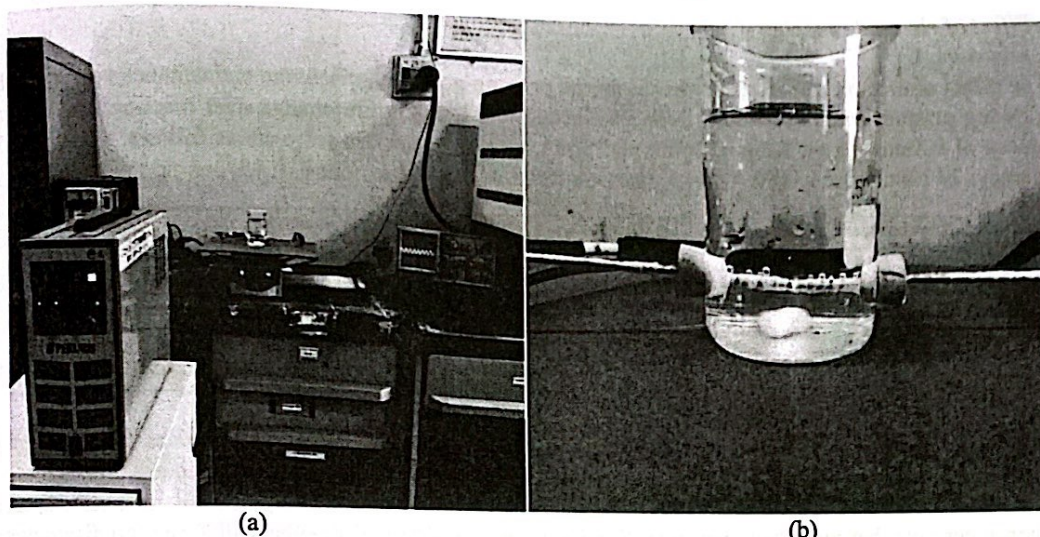
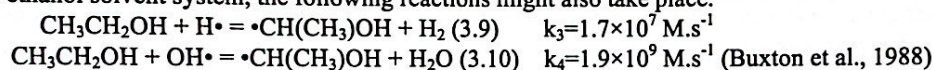


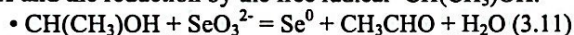
Fig. 1. Synthesis of selenium nanoparticles in distilled water (a) before reaction (b) after 60 minutes

• Water – ethanol solvent

In addition to the creation of free radicals such H, OH, and others during the plasma discharge process in the mixture of water and ethanol solvent system, the following reactions might also take place:



According to the reaction described below, selenium nanoparticles are produced in solution together with the reduction by the free radical H and the reduction by the free radical $\cdot\text{CH}(\text{CH}_3)\text{OH}$.



Since k_4 is significantly bigger than k_3 and the reaction rate constant of the OH free radical with ethanol and H_2SeO_3 solution is substantially higher, the concentration of OH is increased. The conversion of Se^{+4} to Se^0 is favoured by the concentration of free radicals. As a result, the synthesis process occurs in a solvent of water and ethanol.

Figure 2 displays the absorption wavelength of the solution before and after the plasma process. The post-reaction solution displays a definite absorption peak at max 297 nm, but the H_2SeO_3 solution lacks a UV-Vis absorption peak. This confirms that previous papers and plasma discharge production of SeNPs in solution are consistent (Tran et al., 2016), (Yu et al., 2015), (Anu et al., 2020), (Mellinas et al., 2019).

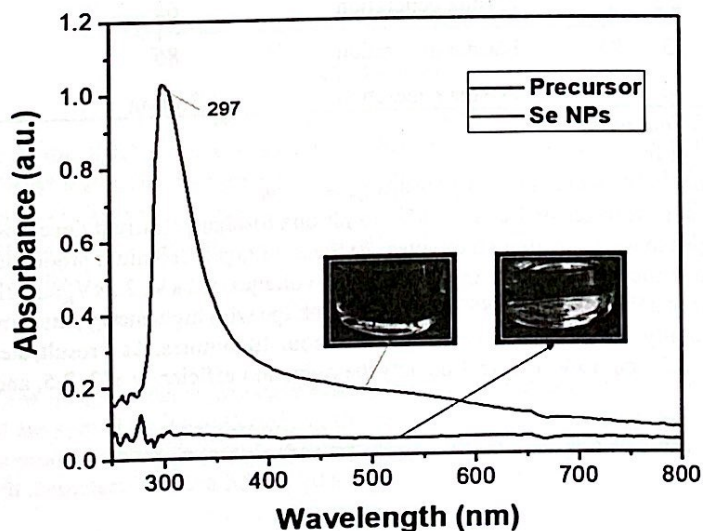


Fig. 2. UV-vis absorption spectrum of the product

As a consequence, this study decides to use a solvent system of water and ethanol in an appropriate volume ratio of 90:10 as a solvent for the plasma solution method of fabrication of selenium nanoparticles.

3.2. Effect of electrode spacing

The effect of electrode spacing on the discharge priming potential, discharge maintenance voltage in the form of glowing plasma, stability of the discharge current, and temperature change over reaction time is studied at distances of 0.5mm, 1mm, 1.5mm, 2mm, and 3mm. Other parameters were set as follows: voltage: 2-3.5 kV, frequency: 20 kHz, pulse width: 0.3 μ s, concentration of H_2SeO_3 solution: 0.01 M; solution pH = 2.5

Table 1. Effect of electrode spacing

Electrode spacing, mm	Spark gap voltage, kV	Stable voltage, kV	Temperature, °C
0.5	2.2	2.0	55
1	2.5	2.0	65
1.5	2.8	2.5	70
2	3.5	3	85
4	Not launched *	Not launched	90

* Formation of electrochemical plasma after 40 minutes.

The findings in Table 1 show that increasing the distance between the electrodes raises the discharge primer potential, discharge maintenance voltage, and reaction solution temperature after 60 minutes. The stability of the plasma current will also alter when the electrode distance is extended due to significant steric effects, leading to discharge currents that may shift over time. Even at electrode distances greater than 3 mm, no discharge plasma forms, but after 30 minutes, electrochemical plasma does.

In order to guarantee the stability of the discharge current and discharge potential when the medium changes throughout the reaction, the research has chosen an electrode spacing of 0.5 mm. Additionally, this promotes in reducing the reaction's temperature rise.

3.3. Effect of voltage

The selenium nanoparticle synthesis process was carried out at different voltages, including 1 kV, 1.5 kV, 2 kV, 2.5 kV, 3 kV, and 4 kV. Table 2 demonstrates the effect of voltage variation.

Table 2. Effect of volatage on synthesis process

Voltage (kV)	Phenomenon	Temperature (°C)	Note
1	No plasma generated	45	-
1.5	No plasma generated	48	-
2	Plasma generation	55	+
2.5	Plasma generation	65	+
3	Plasma generation	85	+
4	Plasma generation	Boiling	*

(-) The reaction did not occur

(+) The reaction occur

(*) Solution was boiled 40 minutes after plasmas generation

Table 2 reveals that at voltages of 1 and 1.5 kV, no plasma discharge current develops in the solution; rather, the solution only begins to warm up after 60 minutes. At these voltages, selenium production does not occur. After 60 minutes, selenium particles begin to form in solution at voltages of 2kV, 2.5kV, and 3kV, with corresponding temperature increases of 55°C, 65°C, and 85°C. At a 4kV voltage with high energy, the temperature of the reaction solution rises substantially, and boiling commences after about 40 minutes. As a result, steady fresh fusion occurs only at voltages of 2, 2.5, and 3 kV. Figure 3 depicts the reduction efficiency at 2, 2.5, and 3kV voltages.

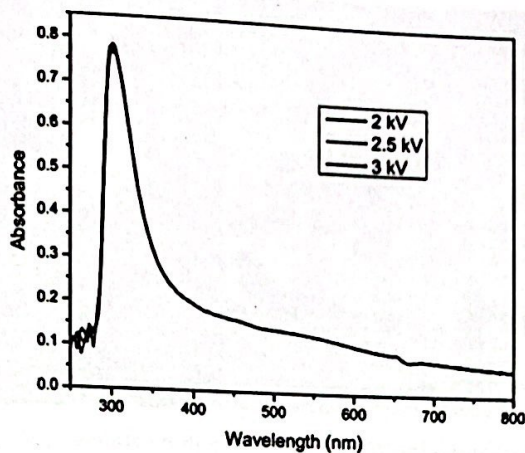


Fig. 3. Voltage's impact on the

efficiency of the reaction

The absorption intensity did not significantly vary period, according to the UV-vis spectroscopy data. As a result, 2kV is the suggested voltage for the reaction process to guarantee thermal stability and lower energy usage.

at voltages of 2, 2.5, and 3kV throughout a 60-min reaction

3.4. Selenium nanoparticles' characterization

3.4.1. XRD results

Figure 3 depicts the X-ray diffraction (XRD) findings of selenium nanoparticle products generated using the solution plasma method

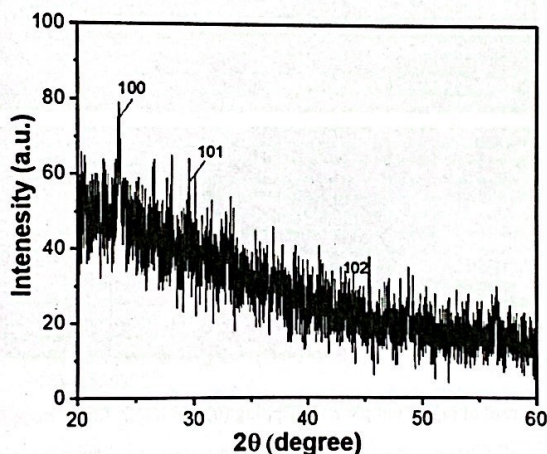


Fig. 4. XRD diffraction of nanoselenium

The figure represents the XRD pattern of triangular phase selenium nanoparticles with lattice constants $a = 4.366 \text{ \AA}$ and $c = 4.956 \text{ \AA}$ that were synthesised using the plasma technique. These peaks are located at 23.5° and 29.7° for the (100) and (100) planes, respectively. The Se nanoparticles created using the solution plasma procedure show low crystallinity in comparison to those created using other processes, according to the diffraction peaks from the XRD sample.

3.4.2. TEM images

Figure 3.10 is a TEM image of the synthesized selenium nanoparticle sample. Selenium particles are present in spherical form and are spread pretty uniformly in the solution with quite comparable sizes, as can be seen in the TEM image of the produced particle sample shown in Figure 5 at 200 nm and 20 nm scales. The particles have little aggregation, with diameters between 50 and 70 nm.

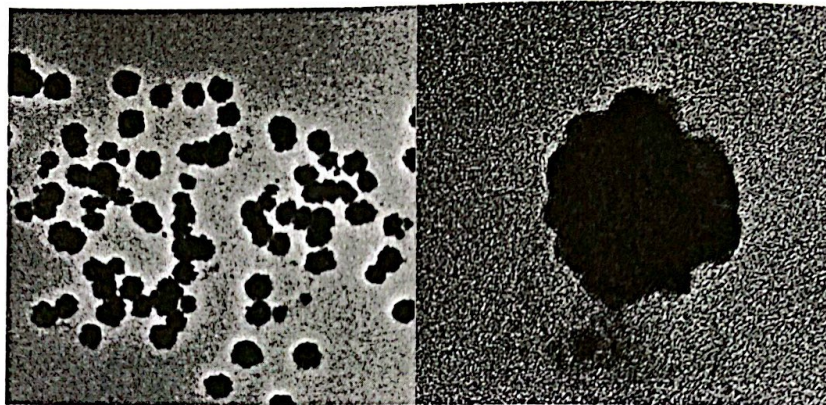


Fig. 5. TEM synthesized

images of

nanoselenium

3.4.3. EDX and particle size distribution results

The samples were examined using the EDX method in order to determine the purity of the substance as it had been manufactured. Figure 6 and Table 3 provide illustrations of the findings.

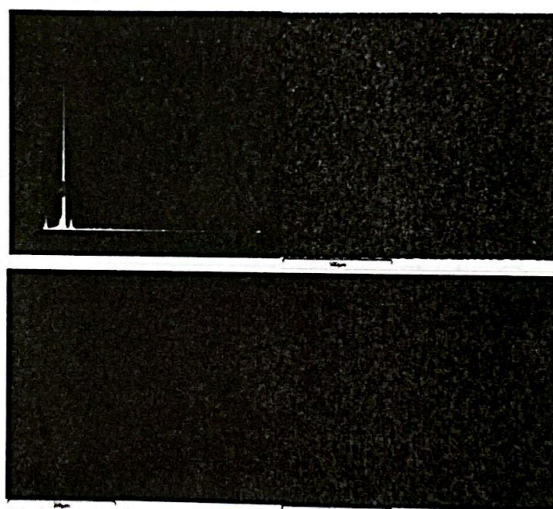


Fig. 6. EDX spectrum of (a) Se sample and mapping (b) of sample, (c) Se mapping and (d) O mapping

Table 3. The elemental composition of the selenium sample

Element	Weight %	Weight % Sigma	Atomic %
O	22.07	0.77	58.30
Se	77.93	0.77	41.70
Total	100		100

Only the elements Se and O are present in the chemical makeup of the selenium nanoparticle sample, as shown by Figure 6 and Table 3, with corresponding composition and mass ratios of 77.93% and 41.70%. The results show that the solution plasma method is capable of producing high purity selenium particles.

Figure 7 displays the typical particle size validated by the particle size distribution (DLS) technique. Figure 7 reveals that the material has spherical granules that are homogeneous in size and well dispersed with an average diameter of 70-90 nm.

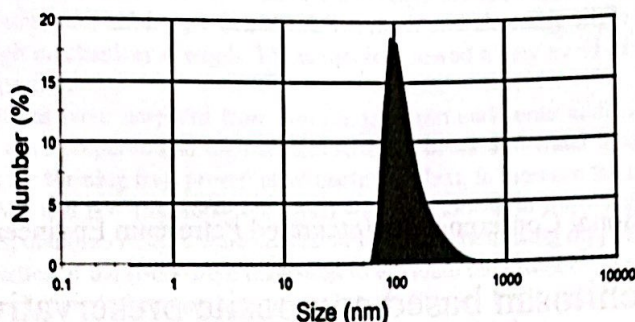


Fig.7. Particle size distribution of as-synthesized nanoselenium

4. Conclusions

Nanoselenium was effectively produced in the study using a novel solution plasma method. The investigations show that a 9:1 combination of ethanol and water is the best solvent for the synthesis process. The additional parameters are as follows: electrode diameter $d = 1$ mm, spacing 0.5 mm, frequency $f = 20$ kHz, voltage $V = 2$ kV, and pulse width 0.3 s. The reaction time is around 60 minutes. XRD, EDX, TEM, and particle size distribution methods were used to evaluate the as-synthesised material, demonstrating the high purity and constant nanosize of 50 to 70 nm of the particles. More study is required to understand the mechanism of action of SeNPs on bacteria, mechanisms of distribution to target areas, and potential hazardous effects on living creatures.

Acknowledgements

This research is funded by Hanoi University of Mining and Geology under grant number T22-11.

References

- Anu, K., Devanesan, S., Prasanth, R., AlSalhi, M. S., Ajithkumar, S., & Singaravelu, G. (2020). Biogenesis of selenium nanoparticles and their anti-leukemia activity. *Journal of King Saud University - Science*, 32(4), 2520–2526.
- Buxton, G. V., Greenstock, C. L., Helman, W. P., & Ross, A. B. (1988). Critical Review of rate constants for reactions of hydrated electrons, hydrogen atoms and hydroxyl radicals ($\cdot\text{OH}/\cdot\text{O}$ —in Aqueous Solution. *Journal of Physical and Chemical Reference Data*, 17(2), 513–886. <https://doi.org/10.1063/1.555805>
- Gao, X., Zhang, J., & Zhang, L. (2002). Hollow Sphere Selenium Nanoparticles: Their In-Vitro Anti Hydroxyl Radical Effect. *Advanced Materials*, 14(4), 290–293.
- Hariharan, S., & Dharmaraj, S. (2020). Selenium and selenoproteins: It's role in regulation of inflammation. *Inflammopharmacology*, 28(3), 667–695.
- Huang, B., Zhang, J., Hou, J., & Chen, C. (2003). Free radical scavenging efficiency of Nano-Se in vitro. *Free Radical Biology and Medicine*, 35(7), 805–813.
- Ikemoto, T., Kunito, T., Tanaka, H., Baba, N., Miyazaki, N., & Tanabe, S. (2004). Detoxification Mechanism of Heavy Metals in Marine Mammals and Seabirds: Interaction of Selenium with Mercury, Silver, Copper, Zinc, and Cadmium in Liver. *Archives of Environmental Contamination and Toxicology*, 47(3), 402–413.
- Kim, S.-M., Cho, A.-R., & Lee, S.-Y. (2015). Characterization and electrocatalytic activity of Pt-M (M=Cu, Ag, and Pd) bimetallic nanoparticles synthesized by pulsed plasma discharge in water. *Journal of Nanoparticle Research*, 17(7), 284.
- Mellinas, C., Jiménez, A., & Garrigós, M. del C. (2019). Microwave-Assisted Green Synthesis and Antioxidant Activity of Selenium Nanoparticles Using Theobroma cacao L. Bean Shell Extract. *Molecules*, 24(22), 4048.
- Sieber, F., Daziano, J.-P., Günther, W. H. H., Krieg, M., Miyagi, K., Sampson, R. W., Ostrowski, M. D., Anderson, G. S., Tsujino, I., & Bula, R. J. (2005). Elemental Selenium Generated by the Photobleaching of Seleno-Merocyanine Photosensitizers Forms Conjugates with Serum Macro-Molecules That are Toxic to Tumor Cells. *Phosphorus, Sulfur, and Silicon and the Related Elements*, 180(3–4), 647–657.
- Spallholz, J. E. (1994). On the nature of selenium toxicity and carcinostatic activity. *Free Radical Biology and Medicine*, 17(1), 45–64.
- Tran, P. A., O'Brien-Simpson, N., Reynolds, E. C., Pantarat, N., Biswas, D. P., & O'Connor, A. J. (2016). Low cytotoxic trace element selenium nanoparticles and their differential antimicrobial properties against *S. aureus* and *E. coli*. *Nanotechnology*, 27(4), 045101.
- Wang, H., Zhang, J., & Yu, H. (2007). Elemental selenium at nano size possesses lower toxicity without compromising the fundamental effect on selenoenzymes: Comparison with selenomethionine in mice. *Free Radical Biology and Medicine*, 42(10), 1524–1533.
- Yu, S., Zhang, W., Liu, W., Zhu, W., Guo, R., Wang, Y., Zhang, D., & Wang, J. (2015). The inhibitory effect of selenium nanoparticles on protein glycation in vitro . *Nanotechnology*, 26(14), 145703.
- Zhang, J., Hu, X., Yang, B., Su, N., Huang, H., Cheng, J., Yang, H., & Saito, N. (2017). Novel synthesis of PtPd nanoparticles with good electrocatalytic activity and durability. *Journal of Alloys and Compounds*, 709, 588–595.
- Zhang, J., Wang, H., Yan, X., & Zhang, L. (2005). Comparison of short-term toxicity between Nano-Se and selenite in mice. *Life Sciences*, 76(10), 1099–1109.
- Zhang, J.-S., Gao, X.-Y., Zhang, L.-D., & Bao, Y.-P. (2001). Biological effects of a nano red elemental selenium. *BioFactors*, 15(1), 27–38.
- Zhu, M., Niu, G., & Tang, J. (2019). Elemental Se: Fundamentals and its optoelectronic applications. *Journal of Materials Chemistry C*, 7(8), 2199–2206.



Integrated Petroleum Engineering

IPE3

Hanoi, October 6, 2022

ISBN: 978-604-76-2595-6



TRANSPORT PUBLISHING HOUSE

TABLE OF CONTENTS

	Page
1 Le Hong Quan, Nguyen Thai Hop, Le Minh Hieu, Vu Nam Hai, Hoang Anh Duc. Application of sequence stratigraphy methodology in petroleum prospection and exploration in Block 09-1, Cuu Long basin, continental shelf of Vietnam	1
2 Kim Nguyen Pham Thien, Son Hoang Ky, Dung Doan Thi My, Hung Tran Ngoc The, Pascal Millot. Behind Casing Gas Saturation Determination with Pulsed Neutron Logging in Gas-Filled Boreholes and High Temperature Formations – First Application in Offshore Vietnam	9
3 Trinh Song Bien, Nguyen Anh Duc, Pham Tuan Anh, Tran Ha Minh, Chau Dang Khoa, Nguyen Ngoc Tuan Anh. Intergration of rock typing by hydraulic flow unit concept and borehold image log analysis depositional facies enviroment	23
4 Nguyen Lam Anh, Nguyen Quoc Dung, Pham Dai Nhan, Nguyen Van Trung, Nguyen Van Nga. Hydraulic Fracturing Technology In Tight Oil Reservoir - Case Studies From Upper Ologocene Reservoir At White Tiger Field	44
5 Nguyen Thac Hoai Phuong, Nguyen Quynh Huy, Bui Khac Hung, Doan Thanh Dat, Dong Van Hoang. Applying integrated adaptive model and algorithm with priori information of reservoir parameters for well test data interpretation in Bach Ho field, Cuu Long Basin	56
6 Nguyen Bao Trung Anh. Research and application of polyamine as inhibitor in drilling mud system when drilling in active clay-containing formations	64
7 Van Tu Truong, The Vinh Nguyen, Van Thinh Nguyen, Tien Hung Nguyen, Khac Long Nguyen, Tai Nguyen Trong. Oil and Gas Well Stimulation by Hydraulic Fracturing in the Oligocene of Bach Ho Field. Case study: Hydraulic fracturing for well X–MSP10	71
8 Truong Nguyen Huu, Tung Phi Manh, Nguyen Van Trung, Nhan Hoang Thinh. Acid treatment of the Basement formation for improved oil rate: A case study of the producer well in the White Tiger field	83
9 Truong Nguyen Huu, W. Bae, X. Nguyen, Nhan HoangThinh. Effect of Fluid Leak-off on Fracture Geometry during Hydraulic Fracturing: A case study in the Lower Miocene Reservoir, White Tiger Field	91

- 10 **Ngo Huu Hai, Nguyen The Vinh, Nguyen Trong Tai.** Potential for producing hydrogen from depleted gas fields with existing production facilities offshore Vietnam 97
- 11 **Quang Nguyen, Tran Anh Tong, Nguyen The Vinh, Truong Van Tu.** Projected FR-PR Conjugate Gradient Algorithm with Stochastic Simplex Approximated Gradient (StoSAG) for Efficient Waterflooding Optimization 107
- 12 **Tran Duy Ngoc Giao, Ta Quoc Dung, Pham Van Hoanh, Le The Ha, Vu Thiet Thach.** Using updated algorithm to built phase diagram for multicomponent hydrocarbon system 115
- 13 **Nguyen The Dzung, Nguyen Lam Anh.** IOR/EOR research & development for Vietsovpetro Joint venture oil fields 127
- 14 **Nguyen Tran Tuan.** Application of rotary – percussion horizontal drilling technology for methane drainage in Khe Cham coal mine, Quang Ninh, Viet Nam 137
- 15 **Nguyen Hai An, Nguyen Hoang Duc, Le Ngoc Son.** Simulation Study On Enhanced Oil Recovery Integration CO₂ Sequestration In Su-Tu-Den Fractured Basement Reservoir 142
- 16 **Ha-Son NGO, Huu-Thanh LE, Ngoc-Tuan TRAN.** Fabrication of nano Selenium in Solution plasma 154
- 17 **Thuy T. L. Bui, Thuan Dinh Dao, Ngoc-Cong Pham.** Fibroin/chitosan based composite preservatives for longan postharvest preservation 162
- 18 **Canh Nguyen Van, Thang Cong Ngoc, Hung Nguyen Tran, Tuan Le Quang.** Modifying Investigation of Nano-silica Additive for Orientating Applications on Enhanced Oil Recovery 173
- 19 **Tho D. Le, Long T. Nguyen, Tuan N. Tran, Thang N. Cong, Hai T. Ngo, Toan V. Vu, Ha M. Nguyen, Hong T. M. Nguyen, Bao T.T. Nguyen, Huong T.T. Tong.** Characterization and Application of Transparent Wood Fabricated from Balsa Wood 181
- 20 **Linh T.Nguyen, Mai Anh T.Nguyen, Ha T.Bui, Duong V.Le, Lan Anh T.Ha.** Influence of the synthesis conditions on the formation of MSU-Z mesoporous material from Vietnamese kaolin and rice husk 188
- 21 **Ngo H Hai, Tran N Trung, Tran V Tung, Dao Q Khoa, Nguyen T Trung, Hoang K Son, Trieu H Truong.** Anomaly Detection for Centifuge Natural Gas Compressor Using LSTM-Based Autoencoder in Hai Thac – Moc Tinh Field, Offshore Vietnam 197